

# UNIVERSITÄT BONN

## Physikalisches Institut

### Single and Pair Production of Neutral Electroweak Gauge Bosons at LEP

Michael Kobel

*Physikalisches Institut, Universität Bonn, D-53115 Bonn, FRGermany*

*on leave of absence from Fakultät für Physik, Universität Freiburg, D-79104 Freiburg, FRGermany*

*E-mail: Michael.Kobel@cern.ch*

*representing the LEP collaborations at ICHEP-98, Vancouver.*

Recent LEP results on single and pair production of neutral electroweak gauge bosons are reviewed. QED and Electroweak  $\gamma$ -e Compton scattering at LEP covers  $\gamma$ -e center-of-mass energies  $\sqrt{\hat{s}}$  in the range from about 20 GeV to 170 GeV, and leads to single production of on-shell  $\gamma$ , off-shell  $\gamma^*$ , and Z bosons, also known as “Zee” process. The latter two final states have been observed for the first time by the OPAL collaboration, while the measurement of the scattered on-shell  $\gamma$ 's by L3 represents the highest energies at which QED Compton scattering has been studied so far. These processes can be used to set limits on excited electrons. Pair production of  $\gamma^*$  and/or Z at the  $e^+e^-$  center-of-mass energy  $\sqrt{s}=183$  GeV has been studied by the DELPHI, L3, and OPAL collaborations. The combination of these experiments yields the first significant measurement of Z pair production. With more statistics at higher energies, interesting limits on anomalous  $\gamma ZZ$  and  $ZZZ$  couplings can be derived from this process.

Post address:  
Nussallee 12  
D-53115 Bonn  
Germany



BONN-HE-98-05  
Bonn University  
October 1998

# SINGLE AND PAIR PRODUCTION OF NEUTRAL ELECTROWEAK GAUGE BOSONS AT LEP

Michael Kobel

*Physikalisches Institut, Universität Bonn, D-53115 Bonn, FRGermany  
on leave of absence from Fakultät für Physik, Universität Freiburg, 79104 Freiburg, FRGermany  
E-mail: Michael.Kobel@cern.ch*

representing the LEP collaborations

Recent LEP results on single and pair production of neutral electroweak gauge bosons are reviewed. QED and Electroweak  $\gamma$ -e Compton scattering at LEP covers  $\gamma$ -e center-of-mass energies  $\sqrt{\hat{s}}$  in the range from about 20 GeV to 170 GeV, and leads to single production of on-shell  $\gamma$ , off-shell  $\gamma^*$ , and Z bosons, also known as “Zee” process. The latter two final states have been observed for the first time by the OPAL collaboration, while the measurement of the scattered on-shell  $\gamma$ 's by L3 represents the highest energies at which QED Compton scattering has been studied so far. These processes can be used to set limits on excited electrons. Pair production of  $\gamma^*$  and/or Z at the  $e^+e^-$  center-of-mass energy  $\sqrt{s}=183$  GeV has been studied by the DELPHI, L3, and OPAL collaborations. The combination of these experiments yields the first significant measurement of Z pair production. With more statistics at higher energies, interesting limits on anomalous  $\gamma ZZ$  and  $ZZZ$  couplings can be derived from this process.

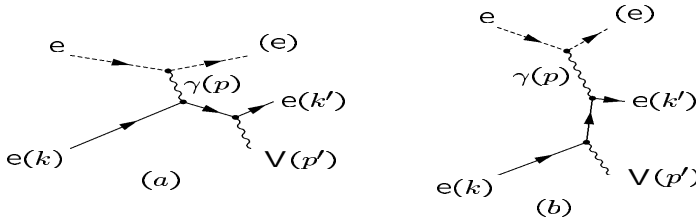


Figure 1: Diagrams for the process  $ee \rightarrow (e)eV$ .

## 1 Single Gauge Boson Production in quasi-real Compton Scattering

The elementary subprocess for the production of a single neutral gauge boson  $V = (\gamma, \gamma^*, Z)$  via Compton Scattering at LEP is  $e\gamma \rightarrow eV$ , where a quasi-real photon  $\gamma$ , radiated from one of the beam electrons, scatters off the other electron  $e$ , as shown in Fig. 1. The electron (e) that radiated the incoming quasi-real photon usually stays unobserved close to the beamline.

For real incoming photons ( $p^2 = 0$ ), the cross-section dependence of the process  $e(k)\gamma(p) \rightarrow e(k')V(p')$  on the Mandelstam variables  $\hat{s} = (k' + p')^2$ ,  $\hat{t} = (k' - k)^2$ ,  $\hat{u} = (p' - k)^2$  is<sup>1</sup>

$$\frac{d\sigma}{d\hat{t}} \propto \frac{1}{\hat{s}^2} \left( \frac{\hat{u}}{\hat{s}} + \frac{2p'^2\hat{t}}{\hat{u}\hat{s}} + \frac{\hat{s}}{\hat{u}} \right). \quad (1)$$

For  $p'^2 = 0$  the well-known terms for QED Compton scattering remain.

### 1.1 QED Compton Scattering, $V=\gamma$

The L3 collaboration has observed 4641 candidate events for the  $e\gamma$  final state produced in QED Compton Scattering<sup>2</sup>, collected in  $230 \text{ pb}^{-1}$  of data taken at  $e^+e^-$  center-

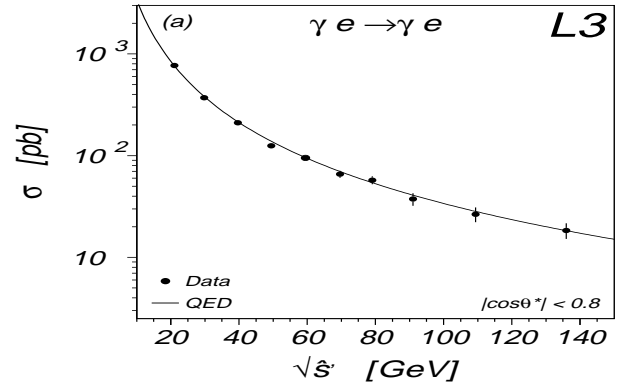


Figure 2: Measured total cross-section of QED Compton Scattering as a function of  $\sqrt{\hat{s}}$ . The solid line shows the QED prediction.

of-mass energies between 91 and 183 GeV. Background from  $e^+e^- \rightarrow e^+e^-$  and  $e^+e^- \rightarrow \gamma\gamma$  has been reduced to below 0.5% by requiring  $E_2$ , the energy of the lower energetic cluster of the  $e\gamma$  pair to be less than 85% of the beam energy. Within  $|\cos\theta^*| < 0.8$  the cross-section as a function of the  $e\gamma$  centre-of mass energy  $\sqrt{\hat{s}}$  has been measured in the range from 20 GeV to 140 GeV, which is the highest energy at which QED Compton Scattering has been studied so far. The measured cross-section is found to be in agreement with the QED prediction (see Fig. 2).

### 1.2 Elektroweak Compton Scattering, $V=\gamma^*, Z$

The production of Z bosons and virtual  $\gamma^*$ 's with a mass  $\sqrt{p'^2} > 5$  GeV decaying to hadronic final states has been studied by the OPAL collaboration<sup>3</sup> using  $55 \text{ pb}^{-1}$  of data taken at an  $e^+e^-$  center-of-mass energy of 183 GeV. The final state is characterized by a single, usually low-energy, electron, isolated from a hadronic

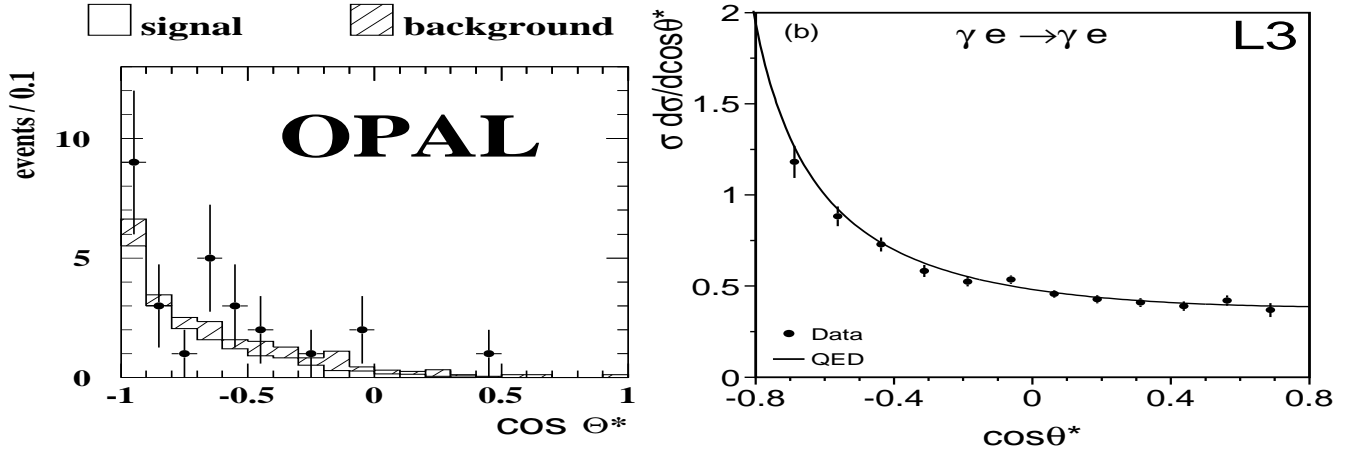


Figure 3: Distributions of  $\cos \theta^*$  for QED Compton scattering (right) and Electroweak Compton Scattering (left).

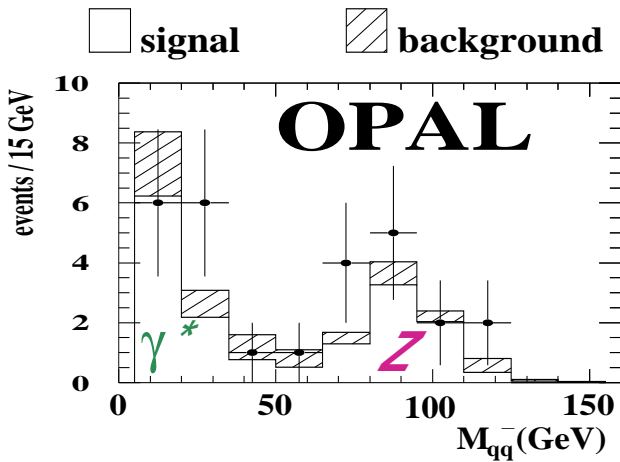


Figure 4: Invariant mass distribution of the hadronic system in candidate events for the process  $e^+e^- \rightarrow (e)e\gamma^*$  and  $(e)eZ$ .

system containing one or two jets from the  $Z/\gamma^*$  decay. The large background of multihadronic  $e^+e^- \rightarrow q\bar{q}$ , semileptonic  $WW \rightarrow qq\nu$ , and especially of events from high  $q^2$   $e\text{-}\gamma$  deep inelastic scattering is greatly reduced by fake electron rejection and by exploiting the distinct signal kinematics, i.e. the scattering angles of the final state particles  $e$  and  $V$ , and the missing momentum due to the escaping electron ( $e$ ) along the beam.

After all cuts, 27 candidate events remain in the data, 14 in a hadronic mass range of  $5 \text{ GeV} < m_{q\bar{q}} < 60 \text{ GeV}$ , dominated by the  $(e)e\gamma^*$  final state, and 13 above 60 GeV, dominated by  $(e)eZ$ . The expected backgrounds are 4.4 and 2.1 events, respectively. The observed significant excess in both mass ranges constitutes the first observation of the processes  $e^+e^- \rightarrow (e)e\gamma^*$  and  $(e)eZ$ . The respective contributions of  $\gamma^*$  and  $Z$  are clearly visible in the hadronic mass distribution, shown

in Fig. 4. The measured cross-section within the detector acceptance is  $(4.1 \pm 1.6 \pm 0.6)\text{pb}$  in the “ $(e)e\gamma^*$ ” region and  $(0.9 \pm 0.3 \pm 0.1)\text{pb}$  in the “ $(e)eZ$ ” region, in good agreement with the predictions of two Monte Carlo generators for this process, PYTHIA and grc4f.

### 1.3 Limits on excited Electrons

The typical transverse momentum of the scattered boson  $V$  is small ( $\hat{u} \rightarrow 0$  in Eq. 1), leading to a dominance of the diagram Fig. 1b. Its kinematics is characterized by a hard spectrum of the boson  $V$ , emitted preferentially close to the initial direction  $\cos \theta^* = -1$  of the scattered electron in the  $e\text{-}\gamma$  rest system, as shown for both, QED and Electroweak Compton scattering, in Fig. 3.

The diagram Fig. 1a could be enhanced by contributions of a hypothetical excited electron  $e^*$ , coupling to  $e\gamma$  and/or to  $eZ$ . This would manifest itself as a peak in the  $\sqrt{s}$  distribution at the  $e^*$  mass. From the absence of such a peak in Fig. 2 the L3 collaboration obtains limits on the free coupling parameter  $\lambda$  in the  $e^*\text{-}e\gamma$  coupling, in units of the electron charge,  $e$ , shown as the solid line on the right-hand plot of Fig. 5. They improve existing limits above the exclusion limit from  $e^*$  pair production.

A hypothetical signal for  $e^* \rightarrow eZ$  in Electroweak Compton Scattering with a production cross-section times branching ratio of 5 pb is shown as dashed line in the left-hand plot of Fig. 5. Quantitative limits for excited electrons decaying to  $eZ, \nu W$ , and  $e\gamma$  are given in another contribution to the conference<sup>4</sup>.

## 2 Pair Production of $\gamma^*$ and/or $Z$ bosons

Neutral current 4-fermion production, where all fermions are visible under large angles to the beamline, is dominated by the so-called “conversion” diagram shown in

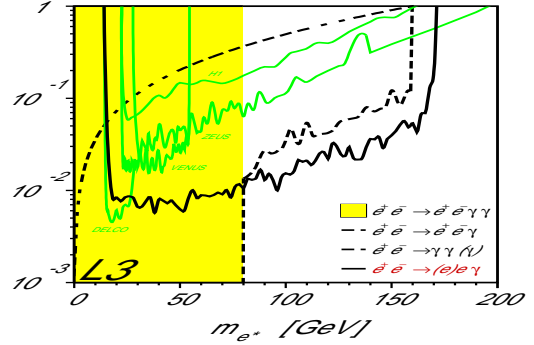
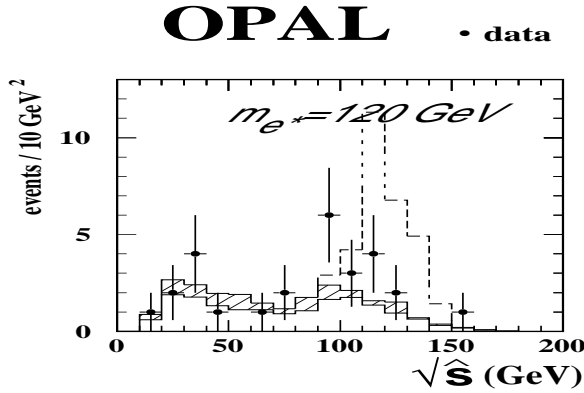


Figure 5: Left-hand side: Distribution of the  $e\text{-}\gamma$  centre-of-mass energy in candidate events for Electroweak Compton scattering. The dashed histogram shows a hypothetical  $e^* \rightarrow eZ$  signal. Right-hand side: Limits in units of  $e$  for  $e^*e\text{-}\gamma$  coupling as a function of the  $e^*$  mass, obtained from QED Compton Scattering.

Figure 6: Pair Production of  $\gamma^*$  and/or  $Z$  bosons.

Fig.6. The data taken at the kinematic threshold of  $\sqrt{s} = 183$  GeV offer the first opportunity to detect on-shell  $Z$  boson pair production via this diagram, by applying mass constraints on the fermion pairs. Some final states of  $Z$  pair production are very hard to separate from the production of a Standard Model Higgs Boson close to the  $Z$  mass. In case of an excess, only a coverage of a large variety of decay channels will help to disentangle Higgs production from possible anomalous  $\gamma ZZ$  and  $ZZZ$  couplings. Inclusive neutral current 4-fermion production without any mass constraints, mainly proceeding via the  $\gamma^*Z$  intermediate state, has been studied in addition. It's observation is an important test for the understanding of higher order processes in the Standard Model, which often constitute a prominent background in the search for new physics.

### 2.1 Inclusive Neutral Current 4-Fermions

The DELPHI<sup>5</sup> and L3<sup>6</sup> collaborations have updated their inclusive studies of Neutral Current 4-fermion events in the final states  $llq\bar{q}$  and  $llll$ , as detailed in Table 1. There is a tendency of observing rather more  $llq\bar{q}$  events than predicted. Since systematic errors have not yet been determined, no statement about the significance of this trend can presently be made.

### 2.2 Selection of $Z$ pair events

$Z$  pair production has been searched for<sup>5,6,7</sup> at  $\sqrt{s} = 183$  GeV in the final states (Branching ratio, experiments)  $qqqq$  (49%, L3 and OPAL),  $qqbb$  (19%, DEL-

Table 1: Preliminary values for number of observed events, expected signal and background for inclusive neutral current 4-fermion processes at  $\sqrt{s}=183$  GeV. Only statistical errors are given.

Channel(Exp.)	$N_{\text{obs}}$	$N_{\text{sig}}$	$N_{\text{bck}}$
eeqq (DELPHI)	3	$2.9 \pm 0.2$	$0.6 \pm 0.2$
$\mu\mu qq$ (DELPHI)	8	$2.9 \pm 0.2$	$0.4 \pm 0.2$
$llqq$ (L3)	13	$7.4 \pm 0.4$	$2.0 \pm 0.1$
llll (DELPHI)	3	$3.7 \pm 0.2$	$0.1 \pm 0.2$
llll (L3)	11	$4.4 \pm 0.1$	$4.2 \pm 0.9$

PHI and OPAL),  $qq\nu\nu$  (28%, L3 and OPAL),  $qqee$  (5%, DELPHI, L3 and OPAL),  $qq\mu\mu$  (5%, DELPHI, L3 and OPAL),  $qq\tau\tau$  (5%, OPAL), and  $llll$  (1%, DELPHI and OPAL). A significant measurement is very difficult, since the expected total cross-section of 0.24 pb for the pure  $ZZ$  diagram is more than 60 times lower than that of  $W$  pair production, the most prominent background for the final states with large branching ratio. On the other hand, the cleaner channels like  $qqee$  and  $qq\mu\mu$  have small branching ratios, so that for each such channel only about 1 event is expected per experiment with the available integrated luminosity of about  $55 \text{ pb}^{-1}$ .

The hadronic channels  $qqqq$  and  $qq\nu\nu$  have been analysed using likelihood techniques and neural nets. DELPHI and OPAL have in addition studied the subsample of  $qqbb$ , where the  $b$ -tag helps in reducing the overwhelming  $W$  pair background. An example of a likelihood distribution for the  $qqbb$  channel from the DELPHI experiment is shown in Fig. 7

In the  $\nu\nu qq$  final state there is important additional background from single  $W$  production,  $(e)\nu W$ , and double initial state radiation return to the  $Z$ ,  $(\gamma\gamma)Z$ , both having even after preselection cuts, cross-sections compa-

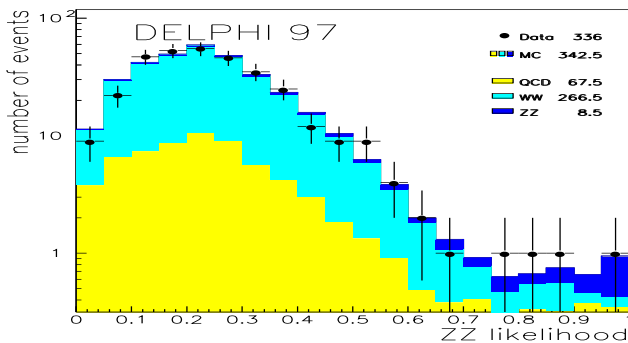


Figure 7: Likelihood distribution for the  $ZZ \rightarrow qqbb$  final state.

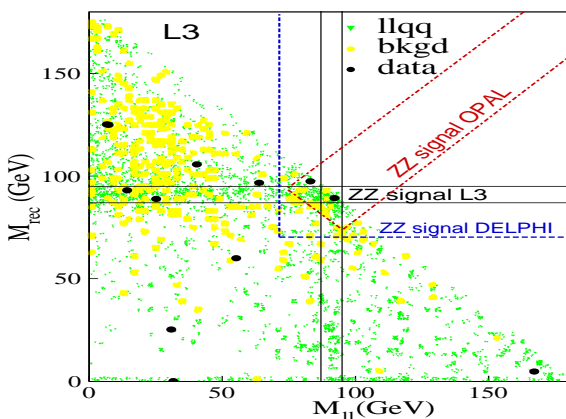


Figure 8: Pair Production of  $\gamma^*$  and/or Z bosons.

rable to the signal. All experiments observe more events in the data than expected from pure background, but — with exception from DELPHI, who apparently profit from a statistical upward fluctuation — the excess is not large enough to significantly claim to have observed Z-pair production from one experiment alone.

### 2.3 LEP average of Z pair cross-section

The average of the observations from the LEP experiments is not straight forward, since very different signal definitions were adopted in terms of the invariant masses of the two fermion pairs. They are indicated in Fig.8, which shows the L3 result for the combined  $eeqq + \mu\mu qq$  final state.

For performing the average I adopted for each channel,  $i$ , the cross-section of the pure  $ZZ$  diagram,  $\sigma_i(ZZ)$ , integrated over the whole phase space, as the signal cross-section to be measured. The theoretical prediction for the sum of all channels,  $\sigma(ZZ) = 0.24$  pb at an average  $\sqrt{s} = 182.7$  GeV, was determined using the YFSZZ gen-

Table 2: Scaling factors for single channel branching ratios, as explained in the text.

channel	DELPHI	L3	OPAL
$llll$	1.40	0.55	0.98
$eeqq$	1.42	0.54	1.01
$\mu\mu qq$	1.05	0.52	0.89
$qqqq$	0.95	0.51	0.86

erator<sup>8</sup>. The number of observed events in the signal region, as defined by each experiment, the selection efficiency<sup>a</sup> within this signal region, and the expected background events were then subjected to a maximum likelihood fit with  $\sigma(ZZ)$  as the only free parameter. The  $qqqq$  and  $qq\nu\nu$  channels of the L3 experiment were excluded from the average, since there the signal had not been defined in terms of the pair masses. Due to large background in these channels their contribution to the average would have been in any case very limited. To perform the likelihood fit, the branching ratio of each channel  $i$  in each experiment  $j$  was scaled by a factor

$$f_{ij} = \frac{\sigma_{ij}(ZZ + Z\gamma^* + \gamma^*Z + eeZ)}{\sigma_i(ZZ)}$$

where  $\sigma_{ij}$  is the expected cross-section for all diagrams leading to the final state  $i$ , (dominated by those listed in parentheses), for the signal definition of experiment  $j$ . The scaling factors obtained from MC predictions for the respective processes are listed in Table 2. Values much lower than unity indicate a restrictive signal definition, while loose signal definitions lead to values larger than unity, especially for eff final states, where a considerable contribution from the  $eeZ$  diagrams of Fig. 1 can enter.

Summed over the three experiments, a total number of 16 candidate events, for about 9 expected background events, went in the fit. The fit results are  $\sigma(ZZ) = 0.63^{+0.31+0.06}_{-0.24-0.02}$  pb for DELPHI, using 4 decay channels,  $\sigma(ZZ) = 0.28^{+0.48+0.10}_{-0.24-0.02}$  pb for L3, using 3 decay channels, and  $\sigma(ZZ) = 0.16^{+0.17+0.03}_{-0.12-0.02}$  pb for OPAL, using 7 decay channels, plus an extra overlap channel between  $qqbb$  and  $qqqq$ . The LEP average yields

$$\sigma(ZZ) = 0.36^{+0.14+0.03}_{-0.12-0.02} \text{pb},$$

constituting the first significant observation of  $ZZ$  production, at a rate consistent with expectation. The re-

<sup>a</sup>DELPHI and L3 have given no numbers for selection efficiencies. They instead give the number of expected signal and background events with statistical errors, only. Their signal definition comprises all neutral current 4-fermion diagrams for each final state within their respective fermion pair mass regions. I estimated their efficiency by determining the corresponding expected cross-sections with the help of the appropriate Monte Carlo Generators. This procedure resulted in relative efficiency errors of  $\mathcal{O}(10\text{--}15\%)$ , assumed to be large enough to cover the missing systematic errors.

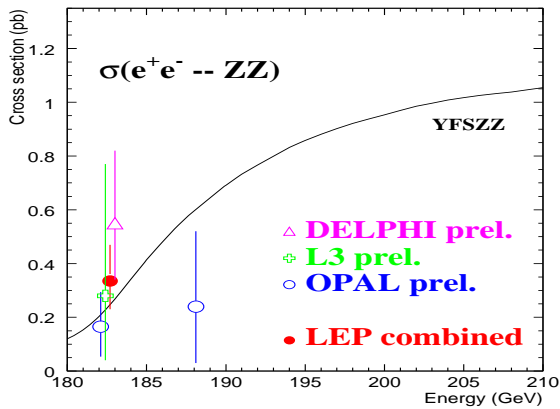


Figure 9: The results of the likelihood fit of ZZ cross-sections. For better visibility a finite distribution of the points along the energy axis is made.

sults are plotted in Fig. 9, where also a preliminary OPAL measurement with the first 40 pb<sup>-1</sup> of data taken at  $\sqrt{s}=189$  GeV is indicated. These very recent data have also been studied by DELPHI<sup>9</sup>, leading results consistent with the Standard Model expectation.

#### 2.4 Anomalous VZZ Couplings (outlook)

For on-shell ZZ production, there are 2 possible anomalous couplings, called  $f_4$  (CP-odd) and  $f_5$  (CP-even) for each, the  $\gamma^*ZZ$  and the  $Z^*ZZ$  vertex<sup>10</sup>. They are zero in tree level Standard Model. Limiting these with more data from LEP2 will pose nontrivial constraints especially on CP violating triple gauge couplings, like non-zero  $Z^*ZZ$  vertices via Higgs loop effects<sup>11</sup>. From Fig. 10 one obtains an impression of the current sensitivity, assuming that the selection efficiency does not depend on the anomalous coupling.

#### Acknowledgements

I would like to thank the organizers of the conference for their hospitality, the representatives of the LEP experiments for their cooperation, and especially David Strom for supplying me with the fitting software.

#### References

1. G. Altarelli, G. Martinelli, B. Mele, and R. Rückl, *Nucl. Phys. B* **262**, 204 (1985)  
E. Gabrielli, *Mod. Phys. Lett. A* **1**, 465 (1986).
2. L3 Collaboration, M. Acciarri *et al.*, CERN-EP 98-109, June 1998, submitted to *Phys. Lett. B*, Contributed Paper # 515 to PA01.

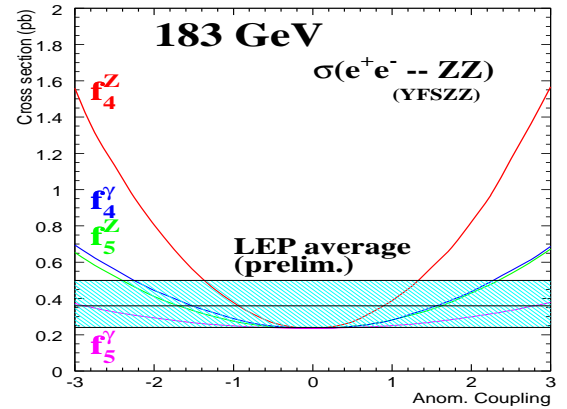


Figure 10: Dependence of the predicted ZZ cross-section as a function of anomalous couplings, and the measured preliminary LEP value.

3. OPAL Collaboration, G. Abbiendi *et al.*, CERN-EP 98-120, July 1998, submitted to *Phys. Lett. B*, Contributed Paper # 265 to PA01.
4. Richard Teuscher, “Heavy and Excited Fermions at LEP”, PA10 talk, Contribution to these proceedings.
5. DELPHI Collaboration, Internal note 98-104, June 1998, Contribution # 230 to PA01.
6. L3 Collaboration, Internal note 2311, July 1998, Contribution # 488 to PA01.
7. OPAL Collaboration, Physics note 363, July 1998, Contribution # 267 to PA01.
8. S. Jadach, W. Placzek, B.F.L. Ward, *Phys. Rev. D* **56**, 6939 (1997).
9. DELPHI Collaboration, Internal note 98-146, June 1998, Contribution # 230 to PA01.
10. K. Hagiwara, R.D. Peccei, D. Zeppenfeld, and K. Hikasa, *Nucl. Phys. B* **282**, 253 (1987).
11. D. Chang, W.-K. Keung and P.B. Pal, *Phys. Rev. D* **51**, 1326 (1995).